COBEM 2021 26th International Congress of Mechanical Engineering
November 22-26, 2021, Virtual Congress, Brazil
ABCM Associação Brasileira de Engenharia e Ciências Mecânicas

COB-2021-0996
INVESTIGATION OF THE PSEUDO-ISOTROPIC APPROXIMATION OF A TURBULENT FLOW IN A STIRRED TANK

Mateus Portella
Process Engineering Department, School of Chemical Engineering, University of Campinas
m184106@dac.unicamp.br

Aline G. De Mitri
Process Engineering Department, School of Chemical Engineering, University of Campinas
a093335@dac.unicamp.br

Helder L. de Moura
Process Engineering Department, School of Chemical Engineering, University of Campinas
helderlima@feq.unicamp.br

Rodrigo de L. Amaral
Department of Mechanical Engineering, Polytechnic School, University of São Paulo
rodrigoamaral@usp.br

José R. Nunhez
Process Engineering Department, School of Chemical Engineering, University of Campinas
nunhez@unicamp.br

Guilherme J. de Castilho
Process Engineering Department, School of Chemical Engineering, University of Campinas
guijcas@unicamp.br

Abstract. *The fluid dynamics study of the turbulent flow in a stirred tank is significantly relevant for optimizing the agitation system, reducing operation costs and improving products, especially in large-scale tanks. In this context, one of the hypotheses generally used for analyzing the turbulence is the pseudo-isotropic approximation, which considers the flow velocity components independent of the evaluation direction. However, the vortices generated by the impeller have a clearly defined orientation, which makes the assumption inconsistent with the phenomena. This work aims to analyze the flow in a stirred tank from the three velocity components (axial, radial and tangential) to investigate the applicability of the pseudo-isotropic approximation. The turbulent flow of water in a tank stirred by a 45º down-pumping pitched-blade turbine operated at 660 rpm using the Stereoscopic-PIV technique was evaluated. Angle-resolved measurements were taken at the fixed blade positions of 0º, 30º and 60º and the results are shown in terms of time-averaged velocity components and turbulent kinetic energy fields. The highest velocities were obtained in the axial direction and the lowest in the radial direction. All the velocities in different angle-resolved fields exhibited substantial velocity fluctuations in the trailing vortices and the discharge regions, especially in the case of the tangential component. It was concluded that the pseudo-isotropic approximation is questionable in the impeller vicinity due to the velocity variations and the vortices formation. However, when the region of interest is located far from this area, the approximation is acceptable.*

Keywords: *pseudo-isotropic approximation, stirred tank, pitched blade turbine, turbulent kinetic energy.*

1. INTRODUCTION

The study of fluid behavior in mixing systems is fundamental for characterizing and understand the process of circulation and mixing made in these vessels. It can help not only in the project stage but also in the choice of the most effective impeller for solving process problems, like the material accumulation. One of the most widespread techniques for investigating the flow dynamics is the particle image velocimetry (PIV), which uses one laser beam focusing on tracer particles that follow the fluid movement and allow to record the flow by one or more cameras and to obtain all the velocity components in the interest direction. The PIV technique application presents some variables related to the number of dimensions and velocity components obtained according to the position and number of cameras. Experiments made with only one camera registers a bi-dimensional plane and allow the evaluation of two velocity components (in general, in the axial and radial directions). However, from the same bi-dimensional plane, it is possible to obtain all three velocity

components (axial, radial and tangential) with appropriate reliability level using two cameras in stereoscopic position (Stereo-PIV) (Raffel et al. 2018). The analysis of three velocity components makes the understanding of flow dynamics more complex and minimizes prospective mistakes because of the out-of-plane motion. However, the use of two cameras is more costly either in the experimental procedure or in the data processing.

In experimental studies that only two velocity components are provided, the pseudo-isotropic flow assumption is commonly used, which considers that the velocity components are independent of the measurement direction. This assumption consists of calculating the tangential component by the average of the other two components. Nevertheless, in the turbulent flow of stirred tanks, the drag vortices generated by the impeller have a clearly defined orientation, which makes the approximation unsuitable to the phenomena (Kresta, 1998).

Among all parameters investigated in stirred tank flows, the turbulent kinetic energy (TKE) is highlighted. It can be defined by the average of the fluctuations of all velocity components in one flow cross-section (Westerweel et al., 2013). Khan et al. (2006) compared the estimated turbulent kinetic energy from the three velocity fluctuations with results obtained by applying the pseudo-isotropic assumption. For this purpose, the authors used a Stereo-PIV to obtain the three velocity components and, in the latter case, they considered that the tangential component could be approximated to the average of the other two components. The vessel was filled with water and stirred by a pitched-blade turbine (PBT) with four blades. It was verified that the pseudo-isotropic hypothesis is unreasonable in areas nearby the impeller, where the tangential velocity cannot be satisfactorily approximated by the radial and the axial components.

Chung et al. (2007) evaluated the pseudo-isotropic hypothesis in a flow of a small stirred vessel whereby Stereo-PIV measurements are impracticable. This research group investigated the flow dynamics of water stirred by a PBT impeller with six blades, in the presence or absence of baffles, and evaluated the acentric impeller position. The tangential component reconstruction was made by the combination of PIV measurements in both vertical and horizontal planes. The system with baffles presented a good agreement of TKE fields when comparing the parameters estimated by the pseudo-isotropic assumption and by the three velocity fluctuations. However, the pseudo-isotropic assumption underestimates TKE values in the experiments without baffles and with the acentric impeller because these systems compromise a uniform energy distribution. For this reason, the tangential velocity becomes more significant when compared to the other components. Additionally, Unadkat et al. (2011) made Stereo-PIV measurements in a vessel with water stirred by a sawtooth impeller, focusing on the impeller vicinity. The pseudo-isotropic hypothesis led to an error of 45% on the value of turbulent kinetic energy when compared to the estimative made with the three components. Therefore, the authors concluded that the assumption becomes questionable close to the impeller. In this region, the authors verified that tangential velocity has a high significance in TKE estimation.

In the present work, the Stereo-PIV technique was used to investigate the flow in a stirred tank generated by a pitched-blade turbine to expand and to contribute to the discussions about pseudo-isotropic assumption. Flow fields of the three time-averaged velocity components and their fluctuations were recorded and analyzed to reveal the flow characteristics associated with the hypothesis. These data were further used to estimate and assess the turbulent kinetic energy fields.

2. EXPERIMENTAL SETUP

The system used in this study consisted of a cylindrical acrylic tank with a standard ASME torispherical bottom, equipped with a PBT impeller with four blades angled at 45º and four metallic baffles equally spaced. More details about the dimensions of the vessel, impeller and baffles are provided in Table 1. The impeller rotational speed used was 660 rpm (11 rev/s), and the experiments were carried out with water as the working fluid (specific mass ρ = 998.2 kg/m³ and viscosity $\mu = 1.003 \times 10^{-3}$ Pa. s) in a turbulent flow pattern, evidenced by Reynolds number of 1.76×10^5, higher than 1×10^4.

Table 1. The geometric configuration of the stirred system.

Property	Value
Vessel diameter (T = 2R)	0.38 m
Liquid heigh	T
Impeller diameter	T/3
Clearance	T/3
Number of blades	4
Blades' angle	45º
Number of baffles	4
Baffle width	T/10
Angle between baffles	90º

The data acquisition was performed following the experimental setup described in Figure 1, composed of two identical *FlowSense EO 8M-21* (3312 x 2488 pixels, 5Hz) cameras and one *Nd:YAG* (532 nm, 200 mJ) laser that generated a light sheet with 2 mm thickness. The lens axes of both cameras were arranged, so that Camera 1 was placed at an angle of $\sigma + \beta = 40^o$ with the normal of the object plane, and Camera 2 was placed at $\sigma = 10^o$. Despite the non-usual configuration, the *Scheinmpflug* principle was respected, which means that the collinearity between the object, the lens and the image planes was assured to focus on the object plane (Prasad, 2000). The flow was seeded using silver-coated glass spheres (d_p = 10 μm). The impeller blades were painted black to minimize the laser light reflection. Angle-resolved measurements were made at three fixed blade positions: 0º, 30º and 60º. An encoder enables the synchronization between the laser pulse, impeller movement and the camera trigger. For each blade position, 1000 pairs of images were recorded in both cameras, in double-frame mode, with 100 μs between the frames.

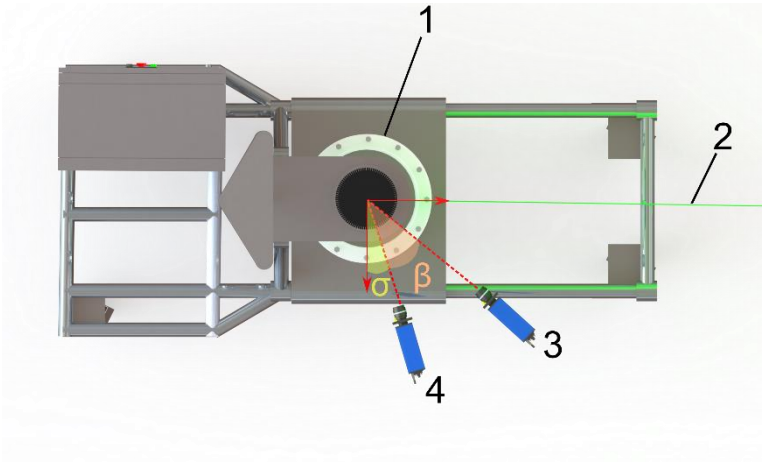

Figure 1. Experimental setup with 1. Mixing system, 2. Laser sheet light, 3. Camera 1 and 4. Camera 2 (Adapted from Barbutti et al., 2020)

Before data acquisition, the system was calibrated using a polymer plate as a target, containing 0.5 mm diameter points equally spaced by 1.5 mm. The cameras obtained the images of the target in the positions described by Figure 1, and the calibration was performed by means of Dantec Dynamic Studio software. The processing of Stereo-PIV measurements was made with MATLAB (MathWorks Inc, version 2018a) software in three distinct stages: pre-processing, processing and pos-processing. In pre-processing, Gaussian filter, subtraction by local minimum and intensity capping filters were applied. In processing, standard cross-correlation (SCC) was implemented and optimized by an iterative multigrid strategy with variations of the interrogation window (Kim and Sung, 2006; Scarano, 2002). In this strategy, the processing was made in four steps. In which step, the interrogation window size was progressively reduced, with a percentage of overlap between neighboring windows. The four steps considered interrogation windows with 48 x 48 pixels, 36 x 36 pixels, 27 x 27 pixels and 20 x 20 pixels, respectively. The overlap between interrogation windows for the first three steps was 25% and for the last one was 50%, resulting in a final area of 10 x 10 pixels. After each step, a simple post-processing based on the work of Westerweel and Scarano (2005) was performed to eliminate outliers. In addition, a complete post-processing based on the mean absolute deviation method (MAD) was applied in the neighborhoods of 3 x 3 interrogation windows (Huber, 2004). The identified outliers by the MAD scale have been eliminated and replaced by values interpolated from a cubic spline (Fritsch and Carlson, 1980).

3. RESULTS AND DISCUSSION

Figure 2 shows the time-averaged mean velocity fields of the radial ($\bar{u}$), axial ($\bar{v}$) and tangential ($\bar{w}$) components normalized by U_{tip} (impeller tip velocity, equals to 4.33 m/s) for the blade angles: AR 0º (a), AR 30º (b) and AR 60º (c). Regardless of impeller position, the flow presented a strongly downward axial pattern due to the movement induced by the down-pumping pitched-blade turbine. Thus, it can be observed that the axial velocity component predominates in the flow, being slightly influenced by the radial component in the suction zone above the impeller. In this region, more expressive values of the radial component were observed. On the other hand, the tangential component showed more significant absolute values in the discharge region, which is attributed to the blade movement. It is important to explain that negative values indicate that the flow direction is into the page.

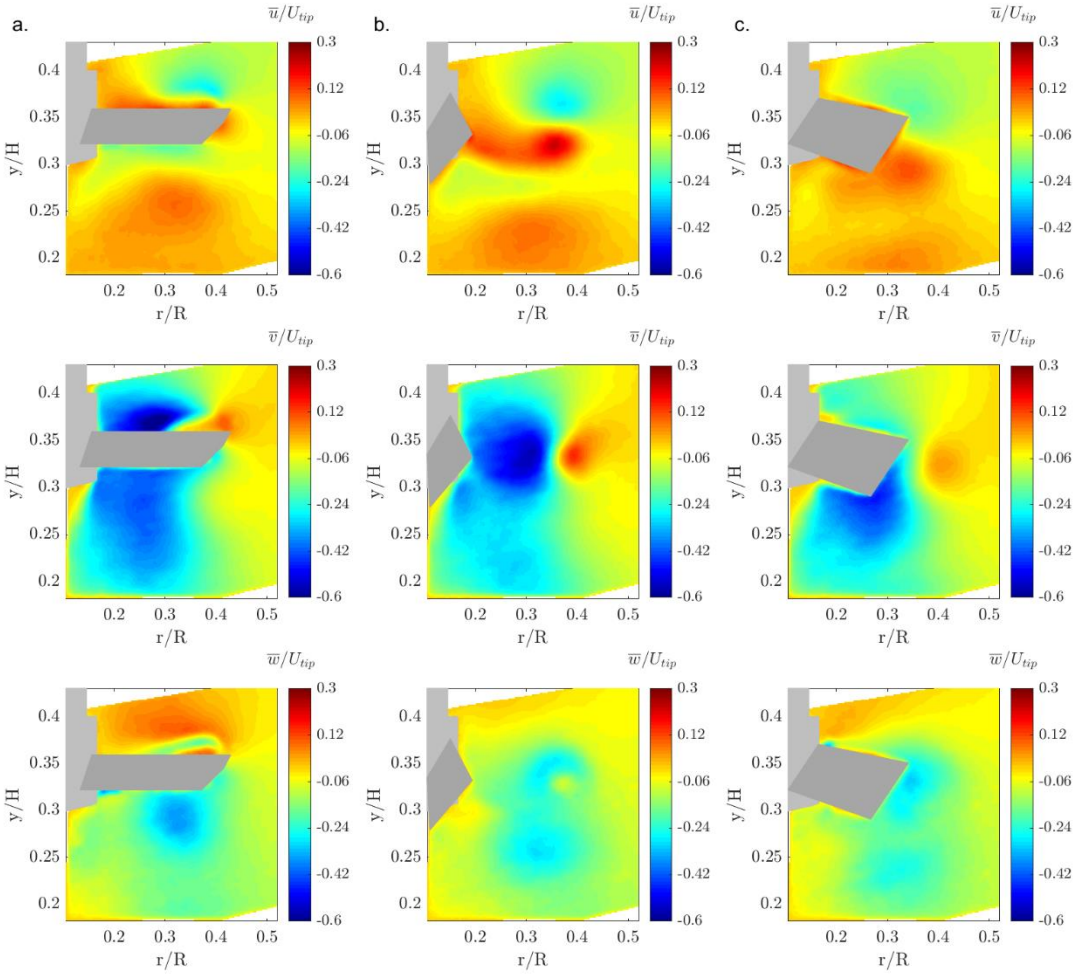

Figure 2. Time-averaged velocity fields from radial ($\overline{u}$), axial ($\overline{v}$) and tangential ($\overline{w}$) components at blade angles (AR) of 0º (a), 30º (b) and 60º (c).

The comparison among the angle-resolved measurements allows verifying that the highest absolute values of the velocity components followed trailing vortices induced by the impeller. It can be observed the movement of the vortices from the suction region at AR 0º to the discharge region at AR 60º, suffering a slight deviation due to the pitched blade. The highest value of the radial component was $0.23U_{tip}$ observed for AR 30º (Figure 2b) in the trailing vortices area (y/H = 0.32 and r/R = 0.35). At the same time, the maximum value of the axial component was $0.65U_{tip}$, identified at AR 0º (Figure 2a) in the suction region (y/H = 0.37 and r/R = 0.28). For the tangential component, the uppermost value was 0.36 U_{tip}, verified at discharge region (y/H = 0.28 and r/R = 0.32) at AR 0º (Figure 2a). The distributions of the velocity components were in agreement with the results of Khan et al. (2006), who observed the trailing vortices detachment between AR 0º and AR 45º when analyzing the flow promoted by the same type of impeller used in this work.

Analyses of the pseudo-isotropic assumption can be done by evaluating the velocity fluctuations fields, which indicate the variation of components in the different flow directions. For the pseudo-isotropic assumption to be considered valid, the fluctuations of the components must present similar values. Figure 3 shows the fields of radial (u'), axial (v')) and tangential (w') velocity fluctuations normalized by U_{tip} for the different impeller positions. It can be observed that the fields of all components present close distributions throughout the analysis region for all angle-resolved measurements. The most expressive fluctuations followed the trailing vortices motion, which means that they moved from the suction region (AR 0º), above the impeller, to the discharge region (AR 60º), under the impeller. However, the fluctuations of the tangential component presented higher values in the trailing vortex zone compared to the other components. The maximum values of u' in this region were $0.26U_{tip}$ (AR 0º), $0.27U_{tip}$ (AR 30º) and $0.23U_{tip}$ (AR 60º), while the maximum v' values were $0.34U_{tip}$ (AR 0º), $0.30U_{tip}$ (AR 30º) and $0.26U_{tip}$ (AR 60º) and the maximum w' values were $0.33U_{tip}$ (AR 0º), $0.35U_{tip}$ (AR 30º) and $0.28U_{tip}$ (AR 60º).

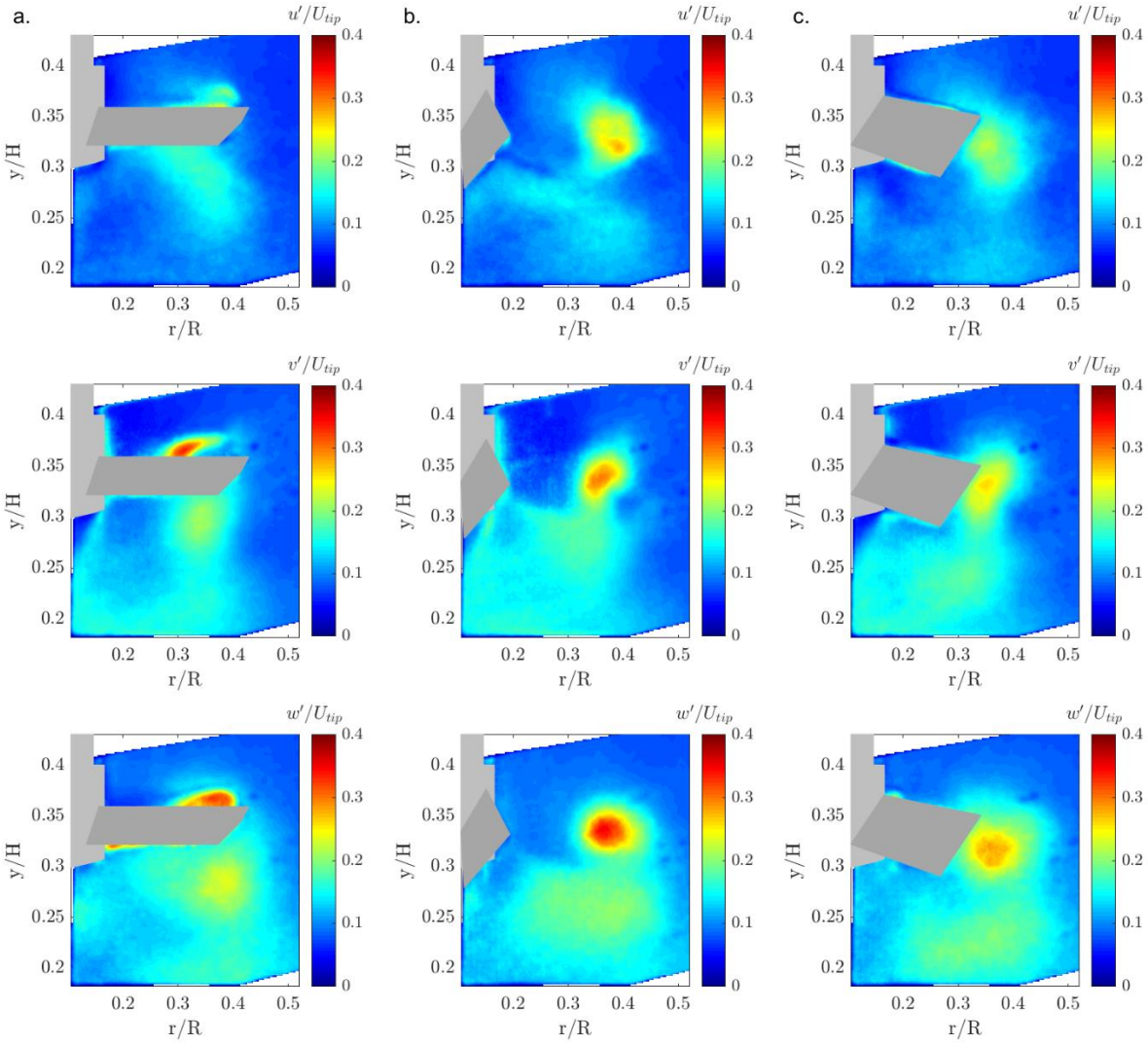

Figure 3. Radial (u'), axial (v') and tangential (w') velocity fluctuations fields at blade angles (AR) of 0º (a), 30º (b) and 60º (c).

The variations among the different directions can be evidenced by analyzing the ratio between the velocity fluctuations. Ratios closer to 1 indicate more favorable situations for the pseud-isotropic assumption. Figure 4 shows the ratio between tangential (w′) and radial (u') components; Figure 5 shows the ratio between tangential (w′) and axial (v') components and Figure 6 shows the ratio between radial (u') and axial (v') components. By analyzing Figures 4 and 5, it is noticed that the ratio tended to be higher than 1 close to the impeller and in the discharge zone. It can be also noticed that the tangential component fluctuations are greater than the other components. Figure 6 indicates that the fluctuations of radial and axial components present closer values, demonstrated by a significant part of the analysis area with ratios closer to 1, except in the suction and in the trailing vortex formation zones. From this analysis, it is possible to affirm that the pseudo-isotropic approximation may be unreasonable for some regions in the flow domain, mainly close to the impeller and in the discharge stream.

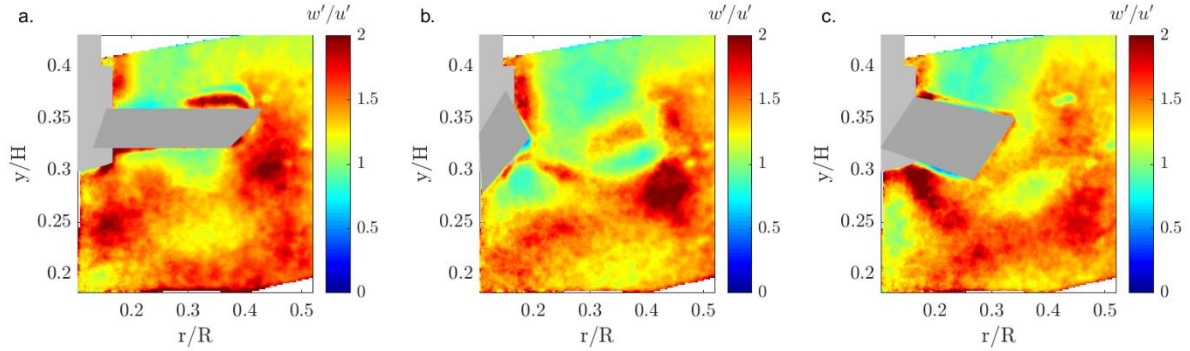

Figure 4. Ratio of tangential (w') and radial (u') velocity fluctuations at blade angles (AR) of 0º (a), 30º (b) and 60º (c).

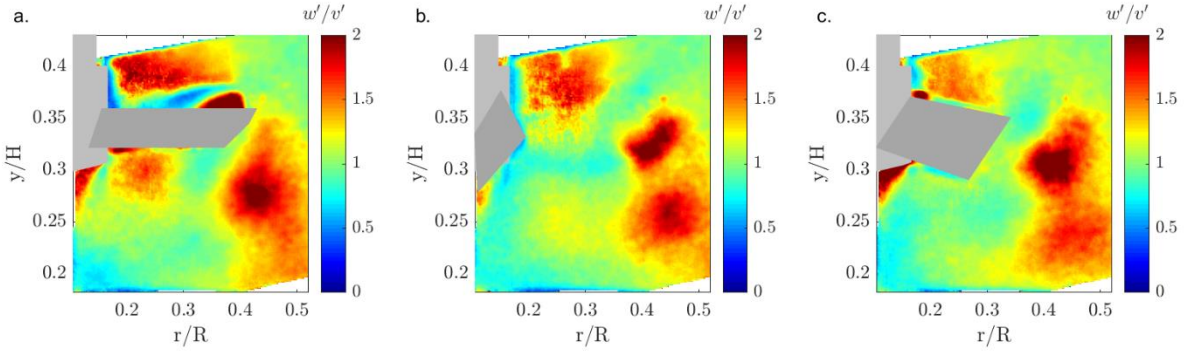

Figure 5. Ratio of tangential (w') and axial (v') velocity fluctuations at blade angles (AR) of 0º (a), 30º (b) and 60º (c).

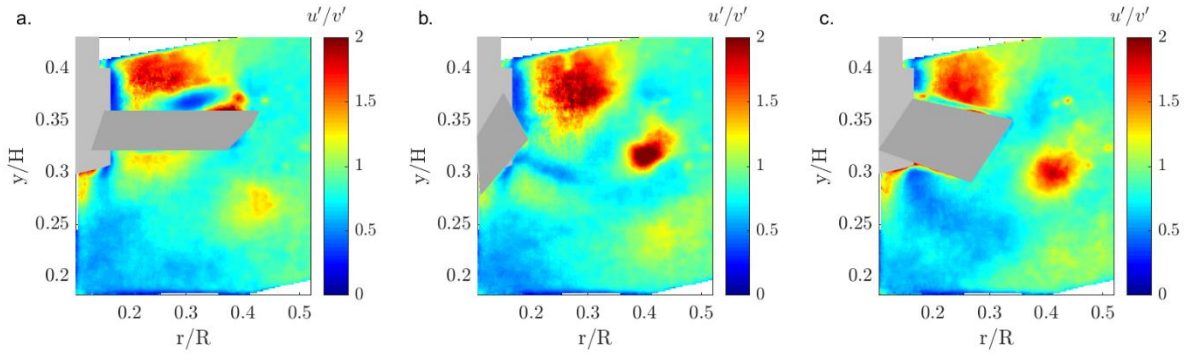

Figure 6. Ratio of radial (u') and axial (v') velocity fluctuations at blade angles (AR) of 0º (a), 30º (b) and 60º (c).

In order to analyze the impact of the differences observed in the velocity fluctuations on the turbulent kinetic energy, this parameter was estimated using both the pseudo-isotropic assumption (Equation 1) and the full definition with all three velocity components (Equation 2).

$$k = \frac{3}{4}(u'^2 + v'^2) \tag{1}$$

$$k = \frac{1}{2}(u'^2 + v'^2 + w'^2) \tag{2}$$

Figure 7 shows the turbulent kinetic energy fields estimated considering the pseudo-isotropic assumption while Figure 8 shows the turbulent kinetic energy fields calculated from the three velocity fluctuations. In both cases, the parameters were normalized by the square of the tip velocity. Regardless of the estimation method, it is clear that the turbulent kinetic energy was concentrated in the region of the trailing vortices formation and followed its movement from the suction region, at AR 0º to the discharge region, at AR 60º.

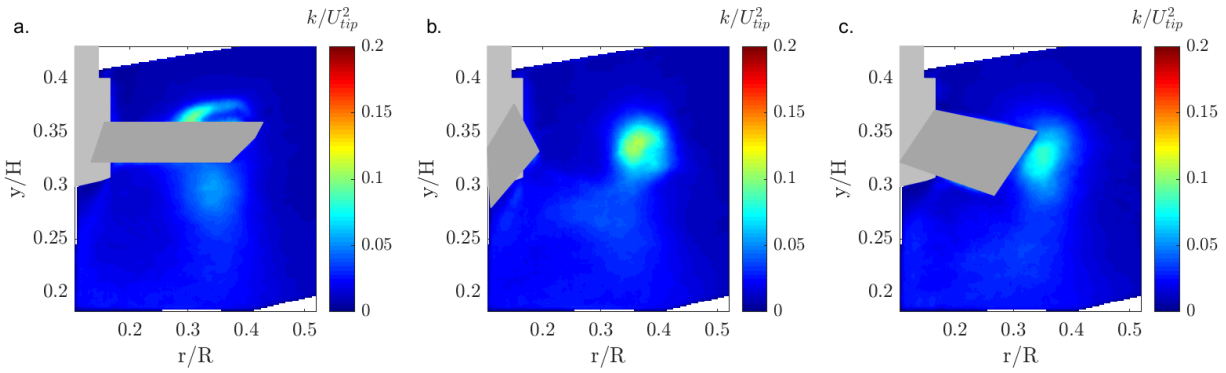

Figure 7. Turbulent kinetic energy fields (k) considering the pseudo-isotropic assumption at blade angles (AR) of 0º (a), 30º (b) and 60º (c).

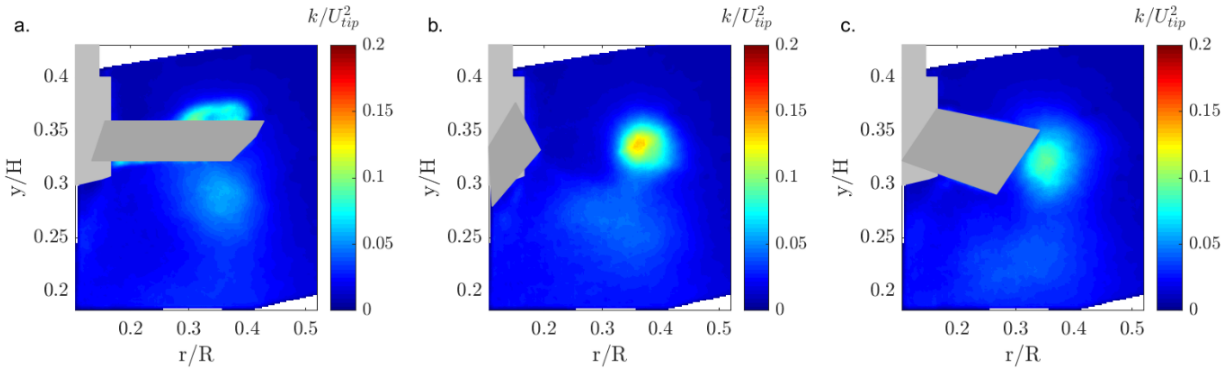

Figure 8. Turbulent kinetic energy fields (k) considering all three velocity fluctuations at blade angles (AR) of 0º (a), 30º (b) and 60º (c).

Comparing the TKE fields, it can be verified that the pseudo-isotropic assumption tends to sub-estimate the TKE values. The highest values of TKE were observed at AR 30º with a maximum of 0.08 U_{tip}^2 for the field estimated using the pseudo-isotropic hypothesis and of 0.13 U_{tip}^2 for the one using all three components. This difference can be associated with the higher values of the tangential component observed in the previous analysis. Thus, the approximation of this component as the average of the other two velocity fluctuations can led to unreasonable values of TKE, especially on the trailing vortices region, where the differences among the tangential, axial e radial components are critical. This observation corroborates with the results of Unadkat et al. (2011), who also verified that the use of pseudo-isotropic assumption sub-estimated TKE values in a flow of a vessel stirred by a sawtooth impeller. Khan et al., (2006) also made these observations regarding the turbulent kinetic energy fields, however, the authors considered that the differences were negligible, and the pseudo-isotropic assumption was adequate. These authors verified lower energy values of the flow induced by the pitched-blade turbine, with a maximum of $0.06U^2_{tip}$ in the discharge region. This deviation may be associated with the fact that they analyzed only the blade position of 0º and, additionally, there are differences between the system geometry, like vessel and impeller diameters.

4. CONCLUSIONS

In this work, Stereo-PIV technique was applied to perform angle-resolved measurements in three different blade angle positions of 0º, 30º and 60º. The results allowed to investigate the application of the pseudo-isotropic assumption on the estimation of the turbulent kinetic energy in a tank stirred by a pitched-blade turbine. Regarding the flow pattern, it was verified that the flow is predominated by the axial velocity component and that it is slightly influenced by the radial component in the suction region. In contrast, the tangential component presented higher values in the discharge region, which is attributed to the blade movement. The comparison between the blade position allowed to observe that the highest absolute values of the velocity components followed the trailing vortices induced by the impeller, which move from the suction region, at AR 0º, to the discharge region, at AR 60º, suffering a slight deviation due to the pitched blade.

The ratios between velocity fluctuations of the different components indicated that the tangential component presents more expressive values than axial and radial components in both the trailing vortices and the discharge regions, regardless of the blade position. The turbulent kinetic energy (TKE) was estimated considering the pseudo-isotropic assumption and compared to that calculated from the three velocity components. It was verified that the TKE was concentrated in the trailing vortices region and its higher values was found for the blade position (AR) of 30º. The pseudo-isotropic hypothesis under-estimated the values of TKE, which are in agreement with other studies on the literature.

In general, it was concluded that the pseudo-isotropic assumption is a valid simplification for estimating turbulent kinetic energy fields but becomes less reasonable in trailing vortices formation regions and in the impeller discharge zone.

5. ACKNOWLEDGEMENTS

This study was financed by Petrobras S/A (process number 2017/00376-1) and National Council for Scientific and Technological Development (CNPq; process number 142604/2019-4).

6. REFERENCES

Barbutti, A.D., De Mitri, A.G., Ayala, J.S., Amaral, R. de L., Moura, H.L. de, Nunhez, J.R., Castilho, G.J. de, 2020. *"Compensation of Image Distortion on PIV Measurements of a Stirred Tank"*. In *Proceedings of the 12th Spring School on Transition and Turbulence – EPTT 2020.* Blumenau, Brazil.

Chung, K.H.K., Barigou, M., Simmons, M.J.H., 2007. "Reconstruction of 3-D flow field inside miniature stirred vessels using a 2-D PIV technique". *Chemical Engineering Research and Design*. Vol. 85, No. 5 A, pp. 560–567.

Fritsch, F.N., Carlson, R.E., 1980. "Monotone Piecewise Cubic Interpolation". *SIAM Journal on Numerical Analysis*. Vol. 17, No. 2, pp. 238–246.

Huber, P.J., 2004. "Scale Estimates". In: *Robust Statistics*. Editora John Wiley & Sons, Inc., Hoboken, New Jersey, pp. 107–126.

Khan, F.R., Rielly, C.D., Brown, D.A.R., 2006. "Angle-resolved stereo-PIV measurements close to a down-pumping pitched-blade turbine". *Chemical Engineering Science*. Vol. 61, No. 6, pp. 2799–2806.

Kim, B.J., Sung, H.J., 2006. "A further assessment of interpolation schemes for window deformation in PIV". *Experiments in Fluids*. Vol. 41, No. 3, pp. 499–511.

Kresta, S., 1998. Turbulence in stirred tanks: anisotropic, approximate, and applied. *The Canadian Journal of Chemical Engineering*. Vol. 76, No. 3, pp. 563–576.

Prasad, A.K., 2000. Stereoscopic particle image velocimetry. *Experiments in Fluids*. Vol. 29, No. 2, pp. 103–116.

Raffel, M., Willert, C.E., Scarano, F., Kähler, C.J., Wereley, S.T., Kompenhans, J., 2018. *Particle Image Velocimetry*. 3ª ed. Editora Springer International Publishing, Cham.

Scarano, F., 2002. "Iterative image deformation methods in PIV". *Measurement Science and Technology*. Vol. 13, No. 13, pp. 1–19.

Unadkat, H., Rielly, C.D., Nagy, Z.K., 2011. "PIV study of the flow field generated by a sawtooth impeller". *Chemical Engineering Science*. Vol. 66, No. 21, pp. 5374–5387.

Westerweel, J., Elsinga, G.E., Adrian, R.J., 2013. "Particle Image Velocimetry for Complex and Turbulent Flows". *Annual Review of Fluid Mechanics*. Vol. 45, No. 1, pp. 409–436.

Westerweel, J., Scarano, F., 2005. "Universal outlier detection for PIV data". *Experiments in Fluids*. Vol. 39, No. 6, pp. 1096–1100.

7. SPONSIBILITY NOTICE

The authors are the only responsible for the printed material included in this paper.